REVIEWS

Journal of Semiconductors
(2023) 44, 041601
doi: 10.1088/1674-4926/44/4/041601

Layered double hydroxides as electrode materials for flexible energy storage devices

Qifeng Lin[1, 3] and Lili Wang[1, 2, †]

[1]State Key Laboratory for Superlattices and Microstructures, Institute of Semiconductors, Chinese Academy of Sciences, Beijing 100083, China
[2]Center of Materials Science and Optoelectronic Engineering, University of Chinese Academy of Sciences, Beijing 100049, China
[3]State Key Laboratory of Integrated Optoelectronics, College of Electronic Science and Engineering, Jilin University, Changchun 130012, China

Abstract: To prevent and mitigate environmental degradation, high-performance and cost-effective electrochemical flexible energy storage systems need to be urgently developed. This demand has led to an increase in research on electrode materials for high-capacity flexible supercapacitors and secondary batteries, which have greatly aided the development of contemporary digital communications and electric vehicles. The use of layered double hydroxides (LDHs) as electrode materials has shown productive results over the last decade, owing to their easy production, versatile composition, low cost, and excellent physicochemical features. This review highlights the distinctive 2D sheet-like structures and electrochemical characteristics of LDH materials, as well as current developments in their fabrication strategies for expanding the application scope of LDHs as electrode materials for flexible supercapacitors and alkali metal (Li, Na, K) ion batteries.

Key words: layered double hydroxide; flexible energy storage devices; structural designs; electrochemical performances

Citation: Q F Lin and L L Wang, Layered double hydroxides as electrode materials for flexible energy storage devices[J]. *J. Semicond.*, 2023, 44(4), 041601. https://doi.org/10.1088/1674-4926/44/4/041601

1. Introduction

The depletion of fossil-fuel resources and the amplification of the greenhouse effect caused by population growth and urbanization have posed unprecedented threats to the sustainable evolution of human society. In an attempt to overcome these issues, the exploration of environment-friendly, low-cost, and high-performance energy storage devices has garnered considerable research attention in recent decades[1, 2]. However, the safety concerns associated with nuclear energy and the unpredictable and intermittent nature of the resources of wind energy, tidal energy, and solar power production have limited the development of energy storage systems[3, 4]. Owing to their advantages of high energy density, high efficiency, rapid charging and discharging, and flexible combination, portable electrochemical energy storage devices have been widely investigated in recent decades[5].

Supercapacitors have advantages such as high storage capacity, high power density, and safe operation, while alkali metal (Li, Na, K) ion batteries (AIBs) exhibit high specific energy density, high operating voltage, and long-cycle life. Consequently, they have both become the focus of research in electrochemical energy storage[6, 7]. These properties are essential for the development of electronic gadgets and electric vehicles[8]. However, the low energy density of supercapacitors is the largest obstacle to their practical development. In particular, the frequent twisting of flexible supercapacitors causes irreversible capacity degradation. The development and application of AIBs are also hindered by their limited power density[9, 10]. The electrochemical performance of both of these systems depends essentially on the chemical composition and microstructure of the electrode material[11, 12]. Consequently, it is crucial to develop electrode materials with large surface areas, rapid reactivity, high cycling stability, and high electrical conductivity.

LDHs have the advantages of facile synthesis, abundant raw materials, high composition flexibility, and adjustable biocompatibility. In recent years, LDHs have been widely used in electrocatalysts[13–15], sensors[16, 17], flame retardants[18, 19], drug delivery systems[20, 21], and energy storage and conversion devices[22, 23]. LDHs are a class of ionic layered compounds that are composed of positively charged brucite-like hydroxide layers known as anionic clays[23, 24]. The hydrogen bond network among water molecules, anion, and hydroxyl layers and the electrostatic force between the anion and hydroxyl layers have established its stable structure, as shown in Fig. 1[25]. The general formula of LDHs is $[M^{2+}{}_{1-X}M^{3+}{}_X(OH)_2]^{X+}[A^{n-}]_{X/n}\cdot mH_2O$, where M^{2+} and M^{3+} represent the divalent and trivalent metal cations, respectively. The molar ratio of $M^{2+}/(M^{2+}+M^{3+})$, typically between 0.2 and 0.33, is denoted as X, and A^{n-1} represents the interlayer anion. LDHs with diverse physicochemical features can be created by altering the molar ratio of M^{2+}/M^{3+} to produce metal cations with different characteristics and interlayer anions of various types[26–28].

Many studies have examined the preparation process of LDHs and their application in electrocatalysis. However, few reviews have focused on the applications of LDHs in supercapacitors (particularly flexible supercapacitors) and AIBs. To bridge the knowledge gap, this review will begin with a description of the design concepts and reaction mechanism It will then summarize the current research ideas and performance of LDHs as (flexible) supercapacitors and AIB electrode

Correspondence to: L L Wang, liliwang@semi.ac.cn
Received 15 NOVEMBER 2022; Revised 30 NOVEMBER 2022.

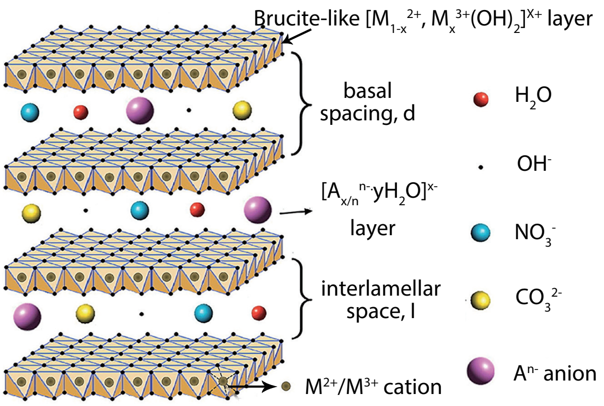

Fig. 1. (Color online) General composition of LDHs[25]. Copyright 2021 , Elsevier Ltd.

materials, as well as the possibilities and problems that they confront.

2. Application of LDHs in flexible supercapacitors electrode materials

Owing to their high power density, extended cycle life, and exceptional temperature stability, supercapacitors stand out among numerous energy storage devices, and thus they have attracted considerable commercial interest[29–31]. Compared with secondary batteries, supercapacitors have higher power densities and are widely used in various high-power equipment, electric vehicles, and energy supply/harvesting devices[32]. However, their low energy density limits their development and application. In addition, with the rapid development of wearable electronic technology, it is difficult to find high-energy-density flexible energy storage materials that provide a stable power output during deformation in flexible supercapacitors to meet the needs of personalized electronic products[33, 34].

Flexible supercapacitors can be divided into electric double-layer capacitors (EDLCs) and pseudocapacitors (PDCs). In general, the specific capacitance and energy density of PDCs are higher than the former. Therefore, various nanostructured pseudocapacitive electrode materials have been widely designed, such as transition metal oxides, hydroxides, sulfides, phosphides, and selenides[35–37]. Compared with other pseudocapacitive electrode materials, owing to their high redox activity, superior interlayer separation, and highly interconnected architecture, LDHs facilitate fast ion transport and reversible redox processes can be used as high-performance electrode materials for supercapacitors with significant growth potential[38, 39]. It is worth mentioning that the factors that affect the pseudocapacitive behavior of different LDHs are the difference in the type of transition metal elements in LDHs, the contact resistance between transition metal elements and OH^-, the electron transfer rate and the interlayer spacing[40].

In this review, we explore the composition of LDHs and discuss the most recent research advancements related to the application of LDHs in supercapacitors (particularly flexible supercapacitors) and the synthesis strategies of electrode materials (Table 1).

2.1. Ni-Co LDHs

Ni-Co LDH is frequently employed as an electroactive material for energy storage owing to its straightforward manufacturing process and the highly reversible reaction capability of the binary combination[41]. The reaction mechanism follows Eqs. (1)–(3)[42, 43]:

$$\mathrm{Co(OH)_2 + OH^- \leftrightarrow CoOOH + H_2O + e^-}, \tag{1}$$

$$\mathrm{CoOOH + OH^- \leftrightarrow CoO_2 + H_2O + e^-}, \tag{2}$$

$$\mathrm{Ni(OH)_2 + OH^- \leftrightarrow NiOOH + H_2O + e^-}. \tag{3}$$

Based on ZIF-67, in which some Co ions were replaced by Ni, Xuan *et al.*[44] developed a hollow-structured Ni–Co LDH on flexible acidified carbon cloth by an in situ growth method (Figs. 2(a)–2(c)), designing a hollow-structured Ni–Co LDH@acidified carbon cloth (H-NiCo LDH@ACC) flexible free-standing supercapacitor active material. The sample with a transfer resistance of 0.15 Ω exhibited a capacity of 1377 mC/cm (3060 mF/cm^2) at 1 mA/cm^2, which is significantly higher than that of H-NiCo LDH@ACF (Fig. 2(d)). Additionally, a 99% coulombic efficiency retention rate and 70% capacity retention rate were still observed after 10 000 cycles at 80 mA/cm^2 (Fig. 2(f)). The PDMS-sealed solid-state H-NiCo LDH@ACC//AC devices assembled under the conditions of 0.0708 mWh/cm^2 energy density and 0.7 mW/cm^2 power density showed no obvious signs of capacity decay after 0°–180° bending (Fig. 2(e)). This is due to the large specific surface area of hollow LDHs, which facilitates charge transfer and ion diffusion and the higher conductivity of the acidified carbon fiber cloth than that of 2D LDHs[44].

Graphene has become a popular topic over the past decade owing to its excellent physical and chemical properties. Because of its high carrier mobility, electrical conductivity, transparency, and mechanical strength, graphene is widely used in flexible supercapacitors[45, 46]. Using a 3D dendritic-cell-nanostructured Ni–Co LDH@rGO as the cathode and wrinkled reduced graphene oxide sheets as the anode, Kiran *et al.*[47] reported a solid-state asymmetric hybrid supercapacitor system (Ni-Co LDH@rGO//crumpled rGO) (Figs. 3(a)–3(b)). The system achieved an energy density of 58.4 W·h/kg and a power density of 3.732 kW/kg at a current density of 0.5 A/g. Figs. 3(c)–3(e) displays the specific performance indicators. The radial alignment of Ni–Co LDHs on rGO improves ion and charge transport, while the dendritic-cell-like morphology offers a broad contact surface for electrolyte entry (Figs. 3(f)–3(h)). Moreover, the large surface area and high electrical conductivity of the crumpled rGO sheets enable the cathode and anode to operate synergistically in order to improve the electrochemical performance of the supercapacitor[47].

Among the various wearable energy storage devices, carbon nanotube yarns are considered to be good candidates for high-performance flexible energy storage devices owing to their inherent mechanical flexibility, high toughness, and good electrical properties[48–50]. In a study by Le *et al.*[51], the pseudocapacitive Ni–Co LDH was wrapped on the surface of a ZnO nanorod forest grown on a carbon nanotube yarn system (Fig. 4(a)). The obtained NiCo-OH/ZnO-NR/CNT-yarn exhibited high electrochemical performance in a three-electrode test system. Furthermore, the symmetric supercapacitor device composed of two NiCo-OH/ZnO-NR/CNT-yarn elec-

Table 1. Performance comparison of LDH-based electrodes for supercapacitors.

Material	Electrolyte	Test method	Specific capacitance/ current density	Capacitance retention (Cycle/current density)	Energy density/ Power density	Ref.
Mn-doped Ni–Co LDH@polyaniline-derived carbon	6 M KOH	All-solid-state flexible asymmetric supercapacitor	1282.06 C/g/ 1 A/g	82.66% (8000th/10 A/g)	78.9 W·h/kg/ 1.55 kW/kg	[58]
Hollow Ni–Co LDH@ acidified carbon cloth	2 M KOH	Flexible free-standing asymmetric supercapacitor	1377 mC/cm^2/ 1 mA/cm^2	70% (10000th/ 80 mA/cm^2)	0.0708 mW·h/cm^2/ 0.7 mW/cm^2	[44]
Ni–Co LDH@rGO	3 M KOH	Asymmetric supercapacitor	2640 F/g/ 1 A/g	80.2% (4000th)	58.4 W·h/kg/ 3.73 kW/kg	[47]
NiCo-OH/ZnO-NR/ CNT-yarn	1 M LiOH	Flexible symmetric supercapacitor	1278 F/g	60.5% (7000th/ 30 Ma/cm^2)	1.38 μW·h/cm^2/ 647 μW/cm^2	[51]
rGO@Ag nanowire/ Ni-Al LDH	6 M KOH	All-solid-state flexible asymmetric supercapacitor	127.2 F/g/ 1 A/g	83.2% (10000th/1 A/g)	35.75 mW·h/cm^3/ 1.01 W/cm^3	[10]
Ni–Fe LDH@rGO@NF	2 M KOH	Flexible asymmetric supercapacitor	1462.5 F/g/ 5 A/g	64.7% (2000th/15 A/g)	17.71 W·h/kg/ 348.49 W/kg	[59]
Co-Al LDH@Ni-Co LDH//CC	6 M KOH	Flexible quasisolid-state asymmetric supercapacitor	2633. 6 F/g/ 1 A/g	92.5% (5000th/4 A/g)	57.8 W·h/kg/ 0.81 kW/kg	[64]
Co–Mn LDH@MnO_2	3 M KOH	Flexible asymmetric supercapacitor	2325.01 F/g/ 1 A/g	95% (10000th/ 30 mA/cm^2)	59.73 W·h/kg/ 1000.09 W/kg	[63]
CC@$NiCo_2Al$ LDH	1 M KOH	Flexible asymmetric supercapacitor	1137 F/g/ 0.5 A/g	91.2% (15000th/5 A/g)	44 W·h/kg/ 462 W/kg	[72]
Zn–Mg–Al LDH@ Fe_2O_3/3D HPCNF	3 M KOH	All-solid-state symmetric supercapacior	3437 F/cm^2/ 1 mA/cm^2	106.5% (40000th/ 50 mA/cm^2)	11.62 mW·h/cm^3/ 9.999 mW/cm^3	[73]

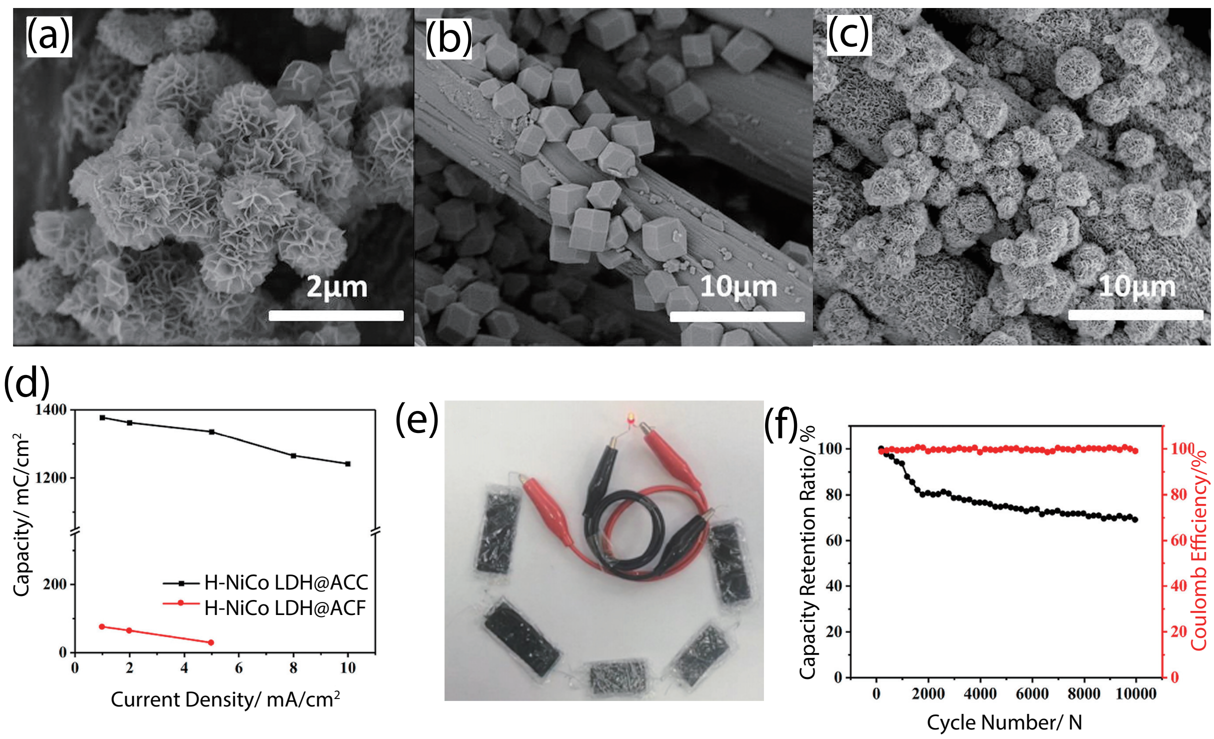

Fig. 2. (Color online) SEM images of (a) H-NiCo LDH powder, (b) ZIF-67@ACC, and (c) H-NiCo LDH@ACC. (d, f) Capacity comparison curve of H-NiCo LDH@ACC and ACF. (e) Optical image of flexible H-NiCo LDH@ACC//AC devices[44]. Copyright 2019, Elsevier Ltd.

trodes exhibited almost no fluctuation in the CV curve when bent to 150°, and the capacitance retention was as high as 75% after 1000 cycles (Figs. 4(b)–4(d)). The excellent performance, strong mechanical flexibility, and reliable cycling characteristics confirmed the feasibility of using flexible fiber-shaped composite yarn materials in wearable energy storage devices[51].

The introduction of heteroatoms into carbon-based materials in recent years has also proven to be an efficient and straightforward means of enhancing capacitance[52–54]. In addi-

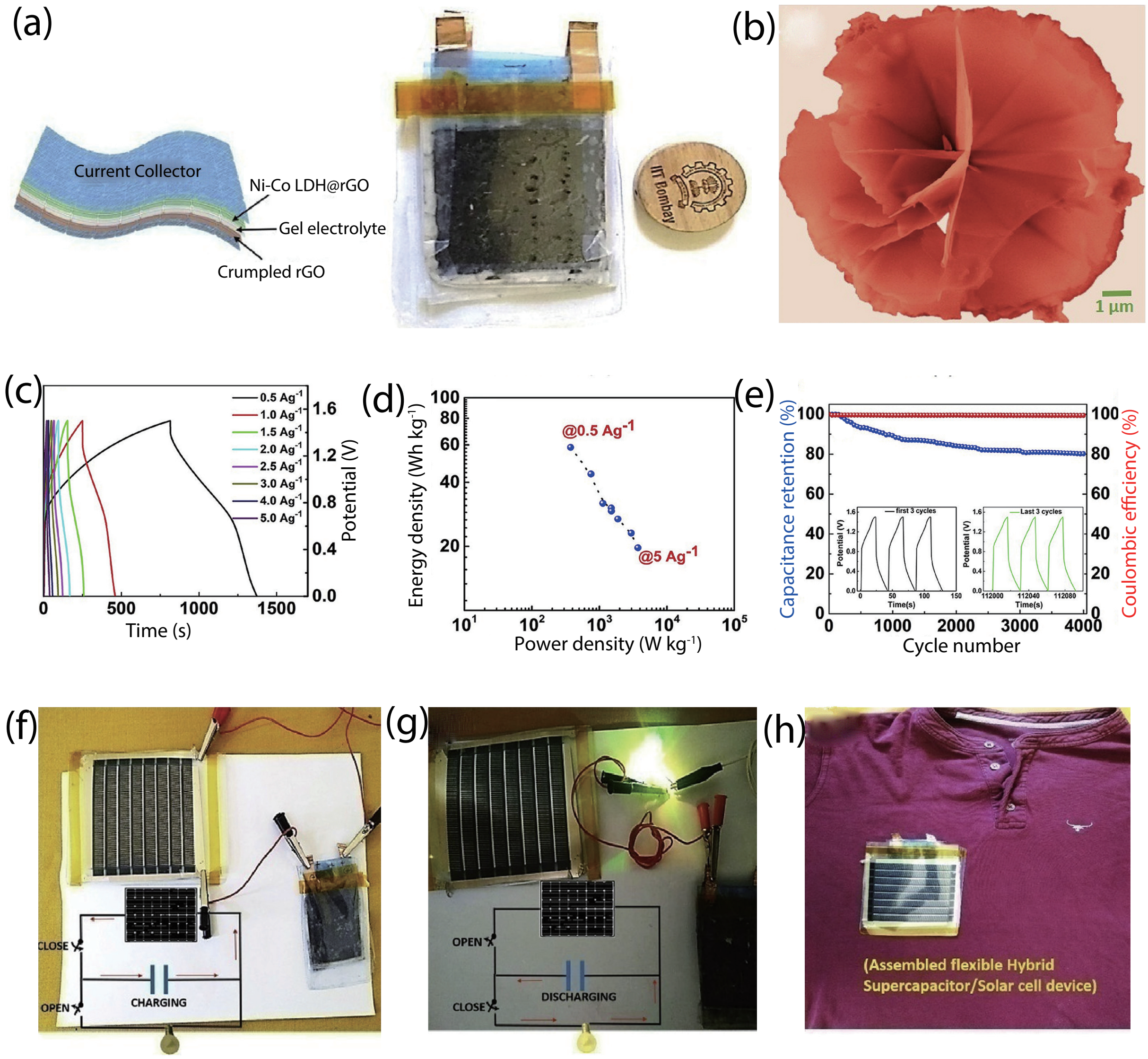

Fig. 3. (Color online) (a) Illustration of flexible Ni–Co LDH@rGO devices. (b) SEM image of 3D Ni–Co LDH@rGO. (c) Charge-discharge curves at different current densities and (d) Ragone plot for the Ni–Co LDH@// crumpled rGO device. (e) Cycle life and Coulombic efficiency curves for the hybrid device. (f–h) Application of flexible Ni–Co LDH@rGO devices[47]. Copyright 2020, Elsevier Ltd.

tion, Mn doping increases the electrode capacity and ion mobility and decreases the surface hydrogen desorption energy[55–57]. In this context, Cao *et al.*[58] deposited Mn ions into NiCo-LDH-nanosheet-coated polyaniline (PANI)-derived carbon (PAC) (Fig. 5(a)), whose specific capacity showed a fourfold increase (from 310.02 to 1282.06 C/g). Furthermore, the flexible all-solid-state asymmetric supercapacitor fabricated with MLDH@PAC as the positive electrode (nitrogen/oxygen self-doped PAC as the negative electrode) exhibited a high energy density of 78.9 W·h/kg under a 1.6-V voltage window and a power density of 1.55 kW/kg. When the curvature changed, and the capacitance retention rate was stable at 82.66% after 8000 cycles (Fig. 5(b)). The experimental results indicate that the introduction of heteroatoms is an effective means of improving the capacitive performance of flexible energy storage devices[58].

2.2. Ni–Fe and Ni–Al LDHs

Iron (Fe) and aluminum (Al) are also used in combination with nickel to form LDHs. Li *et al.* used a two-step electrodeposition method to wrap NiFe-LDHs on reduced graphene oxide (rGO)-modified nickel foam. The prepared Ni-Fe LDHs/rGO/NF composite exhibited a specific capacitance of 1462.5 F/g at a current density of 5 A/g. Moreover, the capacitance retention rate was ~64.7% after 2000 cycles. Additionally, the Ni-Fe-LDHs/rGO/NF-cathode-based flexible asymmetric supercapacitor (mesoporous carbon coated on nickel foam as the anode) displayed a power density of 348.49 W/kg and an energy density of 17.71 W·h/kg. The presence of Fe^{3+} in this system greatly reduced the manufacturing cost in relation to that of the Co-based system[59].

Recently, a novel rGO/silver nanowire (Ag NW)@Ni–Al LDH composite thin-film electrode with a hierarchical core–shell structure has exhibited excellent electrochemical performance. Composites with core–shell structures were formed by growing ultrathin Ni–Al LDH sheets on Ag NWs using the hydrothermal method. Then Ag NW@Ni–Al LDH and rGO were then assembled into GAL hybrid membranes through vacuum filtration (Figs. 6(a)–6(c)). The symmetric all-solid-state flexible supercapacitor (ASFC) prepared with the GAL film as the electrode exhibited a specific capacitance of 127.2 F/g at a current density of 1 A/g, and the capacity retention rate was 83.2% after 10 000 cycles. In addition, the electro-

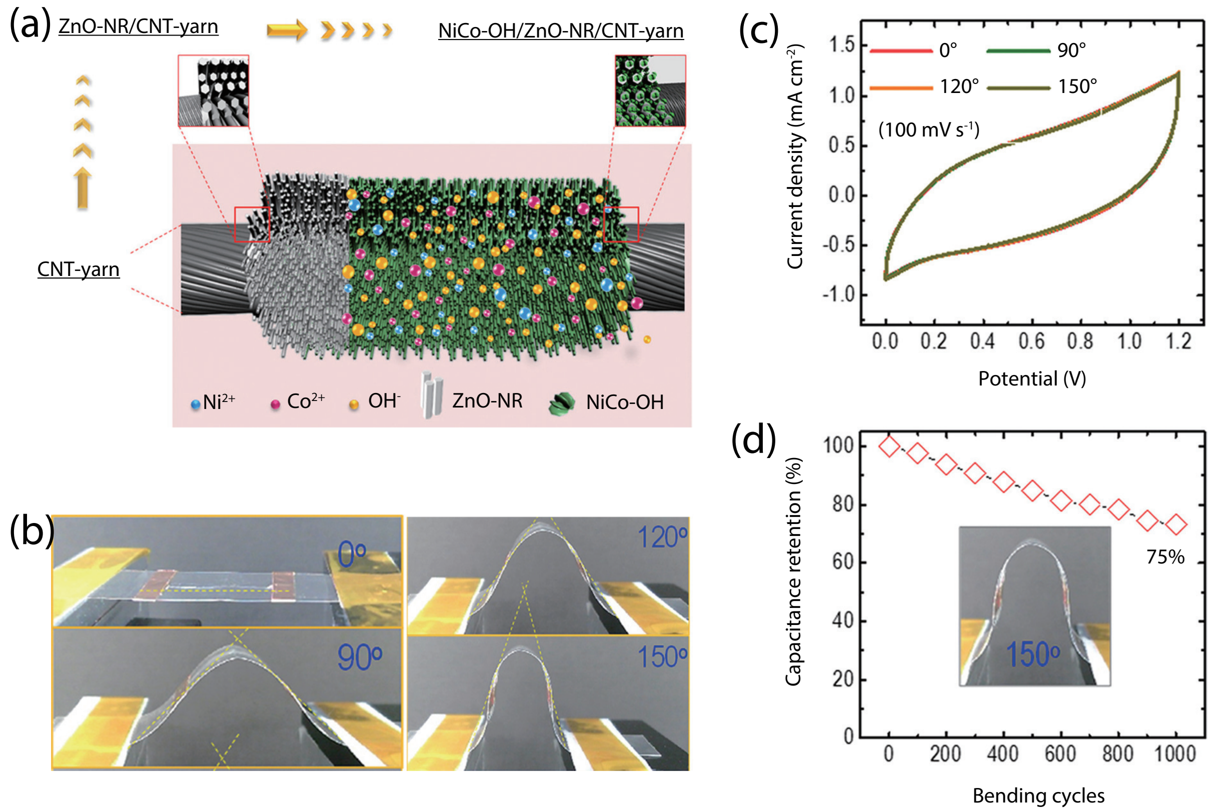

Fig. 4. (Color online) (a) Synthesis schematic of NiCo-OH/ZnO-NR/CNT-yarn fiber. (b) Schematic diagrams and photographs of the bending angles of a symmetric two-electrode supercapacitor device composed of two NiCo-OH/ZnONR/CNT-yarns at each bending angle. (c) CV curves of the symmetric supercapacitor at different bending angles and (d) capacitance retention after 1000 cycles at a bending angle of 150° and the scan rate of 100 mV/s[51]. Copyright 2020, Elsevier Ltd.

chemical performance of the AFSC did not change significantly in the mechanical flexibility test (Figs. 6(d) and 6(e)). This excellent performance is attributed to the remarkable electrical conductivity and mechanical flexibility of the Ag NWs after intercalation in carbon materials, coupled with the pseudocapacitive properties of the high-capacity Al core–shell acting as spacers, which alleviates the aggregation of rGO nanosheets (Figs. 6(f) and 6(g))[10].

2.3. Co–Mn and Co–Al LDHs

Cobalt-based materials have always been attractive electrode materials thanks to their high theoretical capacity and excellent electrochemical performance. However, their actual capacity is often unsatisfactory because of their slow reaction kinetics, short cycle life, and low power density[60]. Recently, a hybrid product of Co–Mn LDH@MnO_2 was grown on nickel foam using a simple hydrothermal method (Fig. 7(a)). The electrode material exhibited an energy density of 59.73 W·h/kg at a power density of 1000.09 W/kg and a specific capacitance of 2325.01 F/g at a current density of 1 A/g in the assembled asymmetric supercapacitors (Fig. 7(b)). The high capacity and energy density benefit from the synergistic effect of the inherent high theoretical capacity of Co-based materials [such as Co_3O_4 (~3560 F/g)] and MnO_2 (theoretical specific capacitance of 1370 F/g)][61, 62]. The excellent capacitance retention (95% capacity retention after 10 000 cycles at 30 mA/cm^2) is attributed to the unique hierarchical structure of the Co-Mn LDH[63]. In addition, these flexible energy storage devices based hybrid material might be as a Power supply platform for wearable system (Figs. 7(c)–7(f))[63].

Inspired by these hybrid-design ideas, Wang *et al.* synthesized a 3D hybrid structure of CoAl-LDH@NiCo-LDH on surface-modified carbon cloth (CC) using a two-step hydrothermal method. Ni–Co LDH nanoneedles grew in situ on the periphery of the Co–Al LDH, and then CoAl-LDH@NiCo-LDH nucleates grew on the modified CC, preventing the undesirable aggregation of LDHs during cycling. Simultaneously, the open area on the surface of the material makes it easier for the electrolyte to penetrate the interior, which improves the ionic conduction efficiency. In this context, flexible asymmetric quasi-solid-state supercapacitors prepared with CoAl-LDH@NiCo-LDH/CC as the positive electrode and active carbon as the negative electrode exhibited energy densities of 57.8 and 38.0 W·h/kg at a power density of 0.81 and 16.09 kW/kg, respectively, under a wide potential window of 1.55 V. The innovation of cobalt-based electrode materials with hybrid architectures represents a new opportunity for future flexible energy storage systems to overcome their performance constraints[64].

2.4. Ternary LDH

In addition to introducing two ions into LDHs, three metal cations have been added to the LDH layer to synthesize one material in recent years, which is also a novel method for improving the extremely flexible ion exchange and composition-tunable features of LDHs[65, 66]. Based on previously reported composites of the Ni-Co LDH with carbon materials[67–69], metal oxides[70], and MXenes[71], Wang *et al.* introduced new concepts and created CC@$NiCo_2Al_X$-LDHs using a surface hydrothermal technique. Fig. 8(a) shows a schematic of the syn-

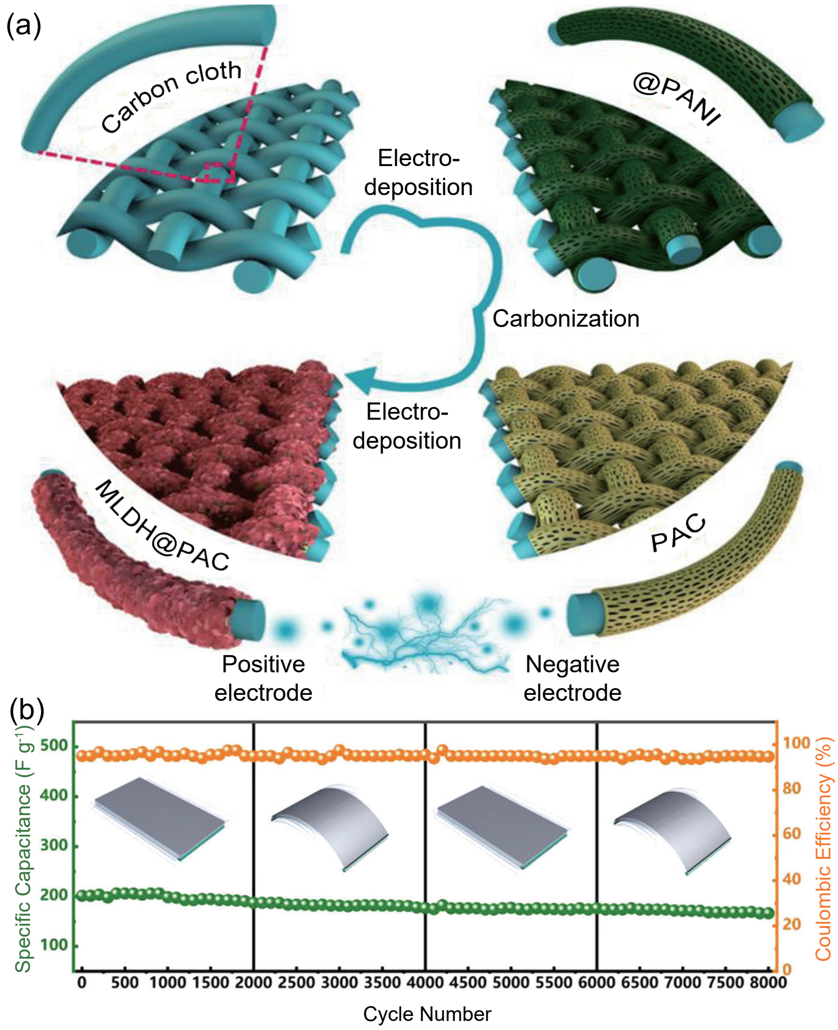

Fig. 5. (Color online) (a) Synthesis sequence diagram of MLDH@PAC. (b) Long-term coulombic efficiency and specific capacity in alternating bend-flat state[58]. Copyright 2019, American Chemical Society.

thesis. Their results indicated that CC@$NiCo_2$Al-LDH exhibited an energy density of 44 W·h/kg at a power density of 462 W/kg and an ultrahigh capacity retention rate of 91.2% after 15 000 charge–discharge cycles. In addition, the capacitor remained stable during large-angle bending (Figs. 8(b)–8(d)). By resolving the bottleneck issue experienced by LDHs, this study offered a novel method for constructing ternary LDHs with strong structures and electrochemical activity (Fig. 8(e))[72].

Kim *et al*. used a hydrothermal process to vertically confine ternary ZnAlMg-LDH (ZMA-LDH) nanosheets and hematite α-Fe_2O_3 nanorods on coaxial electrospun 3D hollow porous carbon nanofibers (3DHPCNF). It is worth noting that ZMA-LDH@Fe_2O_3/3DHPCNF with an appropriate dose of added Zn had a capacity of 3437 mF/cm^2 at a current density of 1 mA/cm^2, and it exhibited superior cycling stability in 40 000 charge–discharge tests (106.5% capacity retention rate). The synergistic impact of three-element or multi-element LDH electrode materials offers promise for overcoming the capacity and stability restrictions of existing flexible energy storage systems[73].

3. Application of LDHs in electrode materials for AIBs

Lithium, sodium, and potassium are members of the IA group and have an outermost electron in the S orbital; hence, their chemical characteristics exhibit obvious homologous behavior[74]. The performance of AIBs is largely determined by the electrode material (Table 2). Scientists have used various methods to improve the performance of the anode material, such as construction of a solid nanoframe structure, elemental doping, and etching to increase the specific surface area and enhance the reaction properties, stability, and conductivity of such materials[75–77]. LDHs with a 2D layered structure can possess one or more of the abovementioned properties after a series of chemical transformations; therefore, they are gradually being widely explored by scientists. In addition, the calcination of LDHs allows the formation of well-dispersed metal oxides with controllable sizes and large surface areas, which can effectively prevent the volume expansion, shrinkage, and aggregation of LIBs during charging and discharging.

3.1. Lithium-ion batteries

Although research on composite materials composed of LDHs and lithium has been conducted for over a decade, the low coulombic efficiency, reversible capacity, and electrical conductivity of such materials limit their further development[78]. Thus, researchers have been attempting to utilize the solid-state electrochemical modification techniques of other metal oxides to construct sophisticated hierarchical nano-

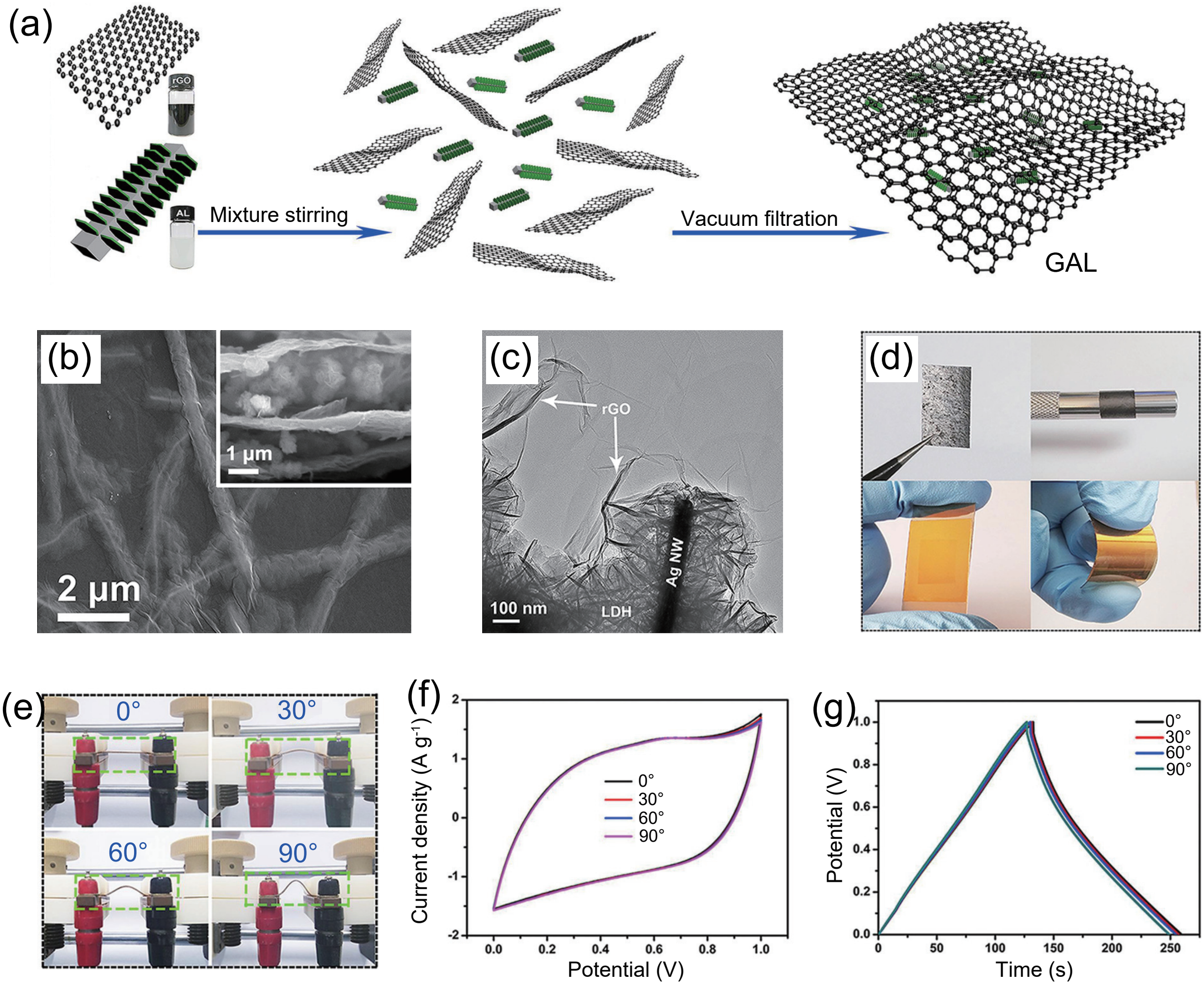

Fig. 6. (Color online) The (a) flow chart, (b) SEM and (c) TEM image of the GAL film. (d) Photographic images of the GAL film and ASFC device. (e) Photographic image, (f) CV and (g) GCD curves of GAL//GAL AFSC device at various bending angles[10]. Copyright 2022, Elsevier Ltd.

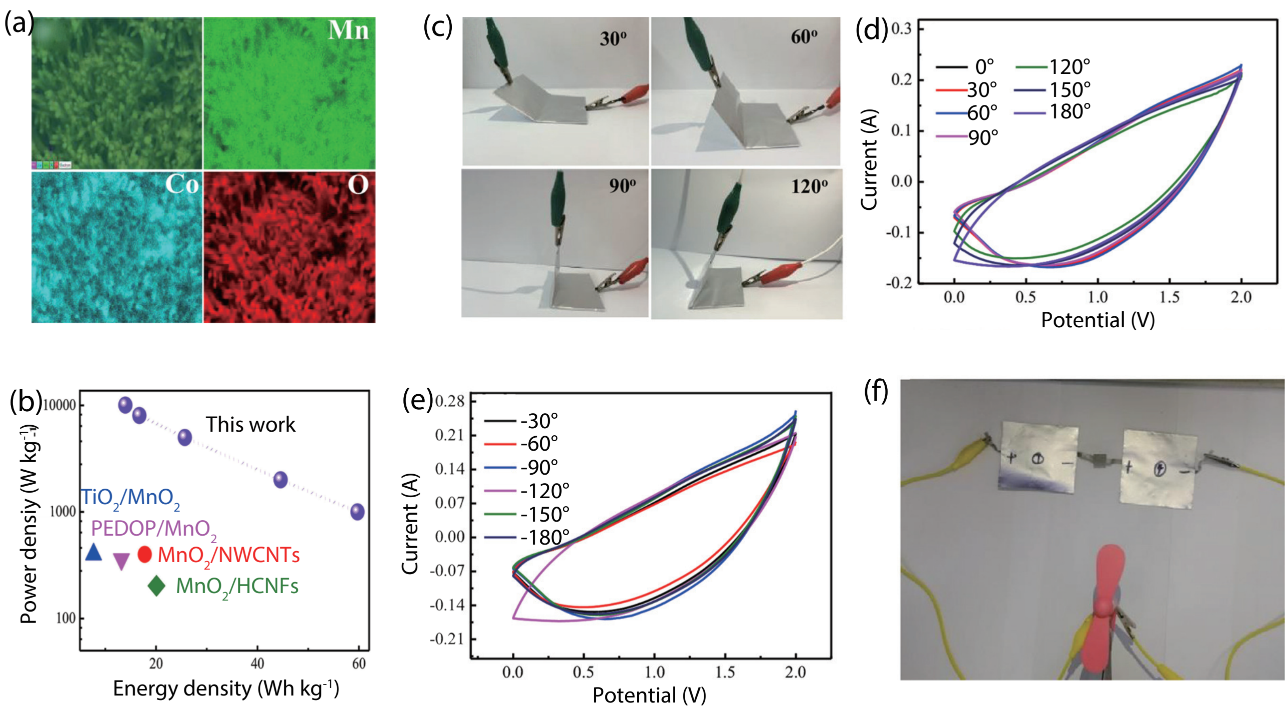

Fig. 7. (Color online) (a) Elemental mapping image of Co–Mn LDH. (b) Comparison of GCD curves of various devices. (c) Optical image of the flexible energy storage devices under bent angles. CV curves of flexible device under (d) 0–180° and (e) –30 to –180°. (f) Optical image of a flexible device unit application[63]. Copyright 2020, Elsevier Ltd.

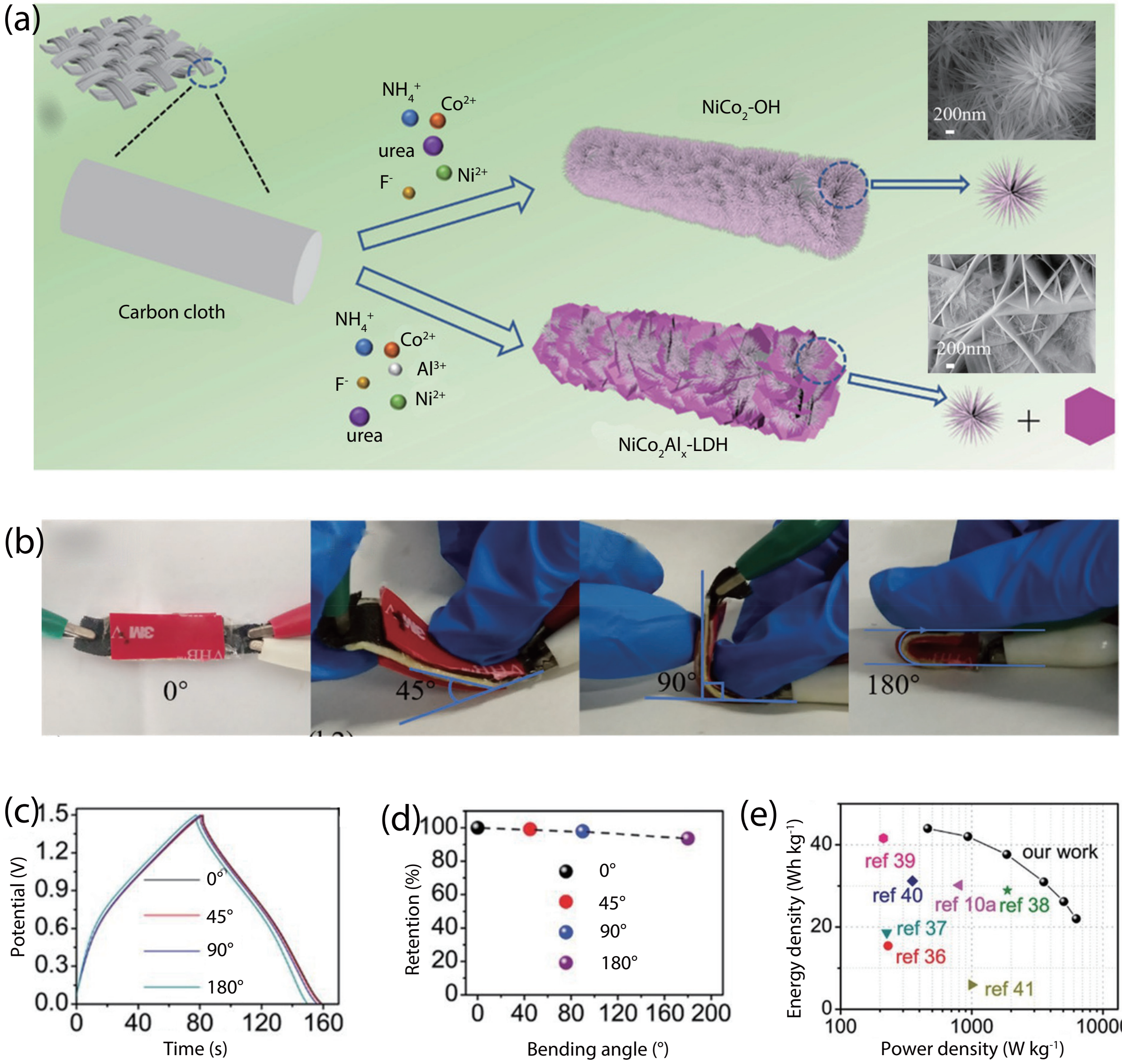

Fig. 8. (Color online) (a) Schematic illustration of the CC@NiCo$_2$-OH and CC@NiCo$_2$Al$_x$-LDH grown on carbon cloth. (b) Photographs of FASC bent at 0°, 45°, 90°, 180°. (c) GCD curves and (d) specific capacitance retention of the FASC at a current density of 2 A/g. (e) Comparison energy density of various energy storage device[72]. Copyright 2019, Wiley-VCH Verlag GmbH&Co. KGaA, Weinheim.

Table 2. Electrochemical performances of various LDHs-based electrode materials in AIBs.

Material	Battery Type	Cycling stability (cycle)/ Current density	Rate performance	Initial coulombic efficiency	Ref.
ZnO/ZnAl$_2$O$_4$	LIBs	1275 mA·h/g (10th)/0.2 A/g	–	–	[80]
Nitrogen and sulfur co-doped porous carbon	LIBs	1175 mA·h/g (120th)/0.5 C	360 mA·h/g at 30 C	–	[81]
CoO/Co$_2$Mo$_3$O$_8$@MXene	LIBs	545 mA·h/g (1200th)/2 A/g	386.1 mA·h/g at 5 A/g	71%	[76]
Multiphase Mn-doped Ni sulfides@rGO	LIBs	206.1 mA·h/g (50th)/0.1 A/g	103.6 mA·h/g at 1 A/g	68%	[82]
Co/(Ni, Co)Se$_2$	SIBs	497 mA·h/g (80th)/0.2 A/g	456 mA·h/g at 5 A/g	80%	[77]
Multiphase Mn-doped Ni sufides@rGO	SIBs	206.1 mA·h/g (2000th)/0.5 A/g	229.2 mA·h/g at 5 A/g	–	[75]
CoFe-NO^{3-}-LDH	SIBs	209 mA·h/g (200th)/1 A/g	228 mA·h/g at at 2 A/g	–	[87]
TiO$_2$ nanoparticles@CNS	SIBs	196.7 mA·h/g (2000th)/2 A/g	197.2 mA·h/g at 10 A/g	41%	[88]
MgFe-LDH	KIBs	371.6 mA·h/g (300th)/0.1 A/g	144.5 mA·h/g at 10 A/g	88%	[94]
CDs@LDH-S	KIBs	188 mA·h/g (8000th)/1 A/g	172 mA·h/g at 5 A/g	–	[95]

structures with excellent structural morphology control and superior performance[79].

As early as 2008, Liu *et al.* demonstrated the growth of Zn-Al-LDH thin films on galvanized stainless-steel substrates at room temperature through the mature thin-film coating technology. Through this approach, ZnAl-LDH was converted to the oxide of the ZnO/ZnAl$_2$O$_4$ composite after calcination at high temperature (650 °C), which was used to synthesize a negative electrode material for lithium-ion batteries (LIBs) for the first time. The test results showed that the discharge

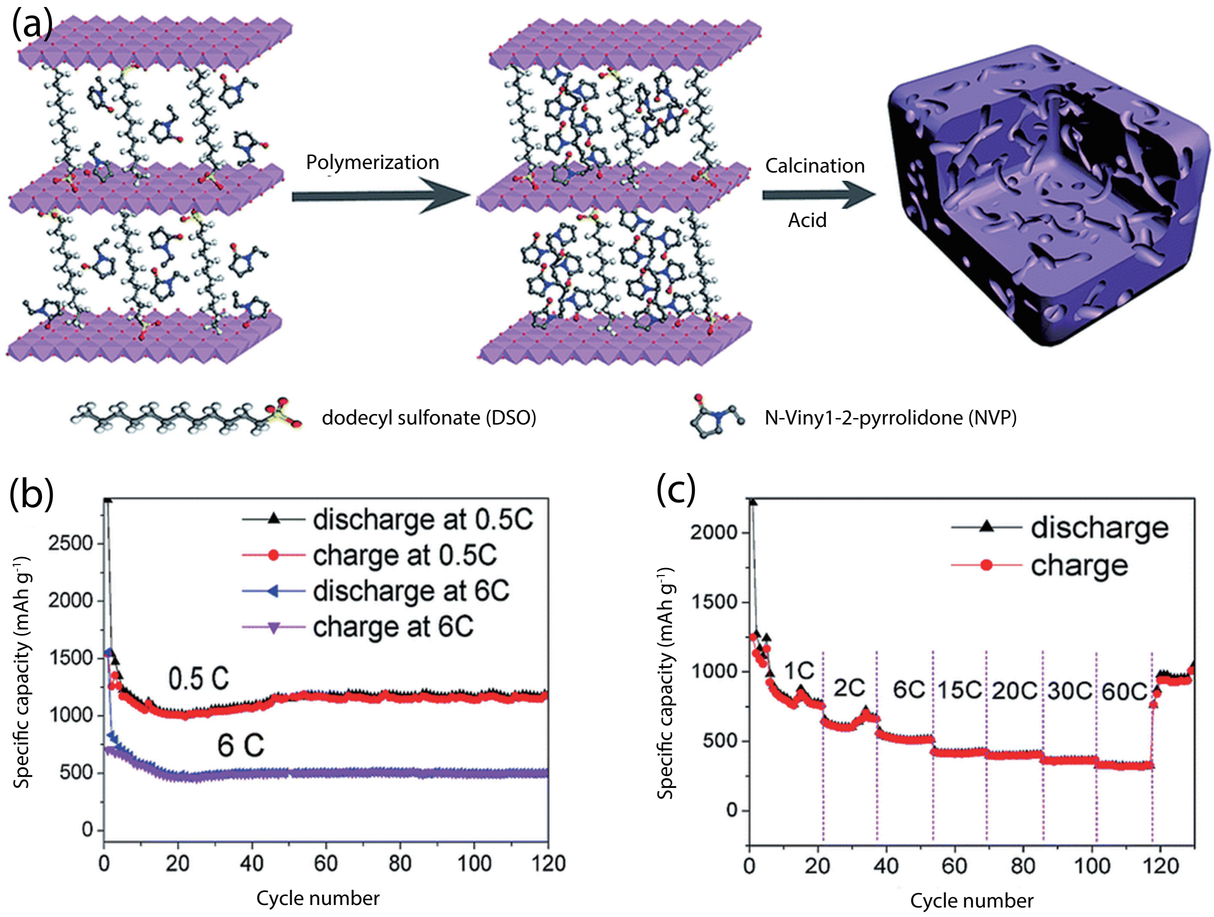

Fig. 9. (Color online) (a) Schematic illustration of the synthesis process of NSPCs. (b) 120-cycle curves at different current density of 0.5 and 6 C. (c) Rate performance curves of NSPCs-800[81]. Copyright 2016, The Royal Society of Chemistry.

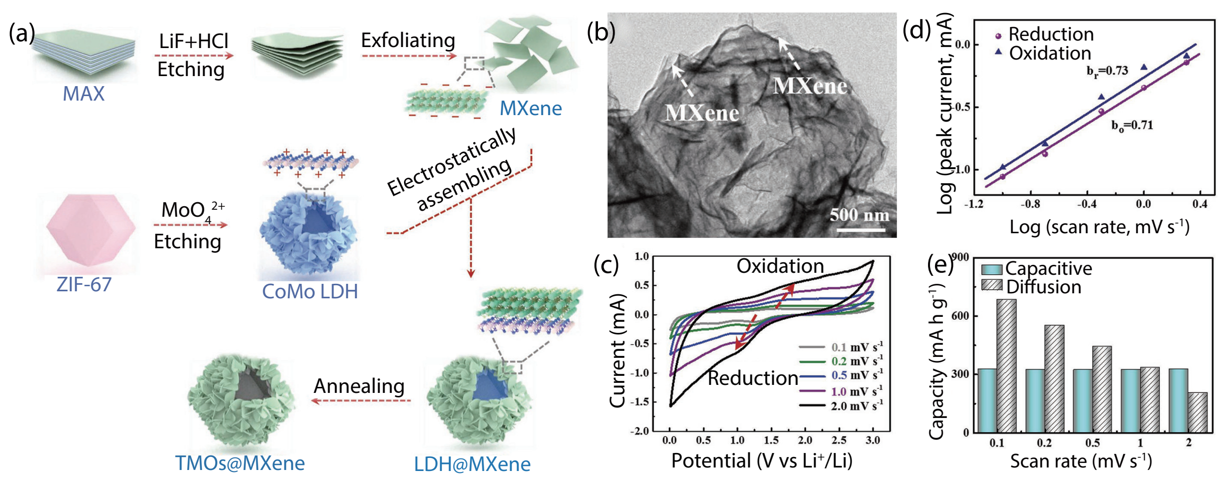

Fig. 10. (Color online) (a) Schematic diagram of TMOs@MXene hollow polyhedron. (b) TEM image of TMOs@MXene hollow polyhedron. (c) Rate performance of pristine $Ti_3C_2T_x$, $CoO/Co_2Mo_3O_8$ and $CoO/Co_2Mo_3O_8$@MXene anodes. (d) $CoO/Co_2Mo_3O_8$@MXene's 1200 cycle stability curve under 2 A/g[76]. Copyright 2019, Wiley-VCH Verlag GmbH&Co. KGaA, Weinheim.

capacity of the $ZnO/ZnAl_2O_4$ porous nanosheets reached 1275 mA·h/g in the first cycle and stabilized at 500 mA·h/g after 10 cycles. $ZnO/ZnAl_2O_4$ has better electrochemical properties than pure ZnO (Fig. 9(a)). This is attributed to the uniform distribution of $ZnAl_2O_4$ in the ZnO particle grid, which effectively mitigates the phenomenon of energy attenuation during charging–discharging. The research results provide unlimited possibilities for the development of LDH-based anode materials[80].

Subsequently, Zhang *et al.* fabricated nitrogen and sulfur co-doped porous carbon materials (NSPCs) using the 2D interlayer confinement effect of the LDHs. It is worth noting that the authors confined organic molecular precursors to the interlayer of LDHs, and at the same time replaced a part of the aluminum ions in Mg-Al LDHs with catalytically active iron ions. The yield of the desired product is increased; the degree of graphitization of the material is enhanced; and the construction of a porous structure is promoted. Finally, the addition of N and S introduces many edge defects into the material, and the micropores formed by these defects can be used

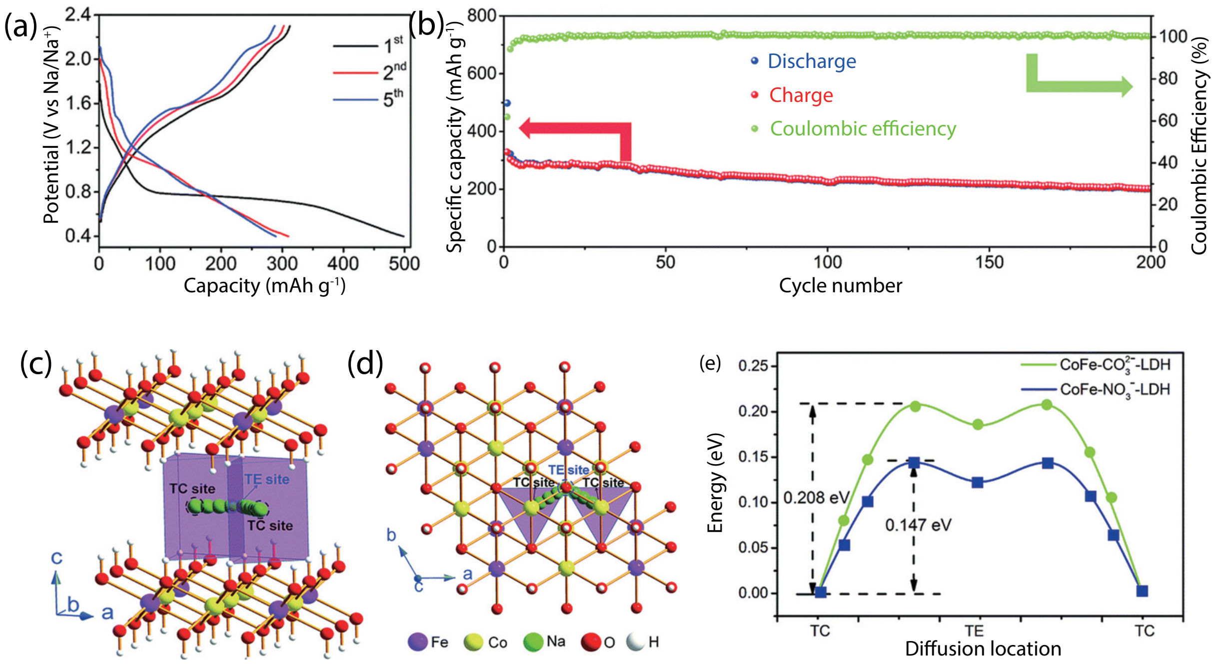

Fig. 11. (Color online) (a) The charge-discharge capacity curve at the 1st, 2nd, and 5th laps and (b) cycling performance of CoFe-NO_3^--LDH at 1 A/g. The (c) side view and (d) top view of Na migration model diagram. (e) The diffusion barrier profiles for Na migration along the path TC→TE→TC[87]. Copyright 2019, The Royal Society of Chemistry.

as active sites for lithium-ion storage. It is precisely because of the existence of these micropores and mesopores that the specific surface area of the material is as high as 1493.2 m^2/g. This structure maintains ultrahigh stability of 1175 mA·h/g after 120 cycles at 0.5 C current density, and exhibits satisfactory cycling stability in the rate performance test with large gradient current density changes (Fig. 9(b))[81].

In addition to lamellar structures, LDHs can be synthesized into hollow nanocages. Lu *et al.* prepared a hollowed Ni-Co LDH polyhedron H-(Ni, Co)-LDHP) using a sacrificial template method. The hollow structure had a large specific surface area and good permeability, allowing the generation of numerous active sites and promoting charge transfer; its capacity reached 928.3 mA·h/g under 0.1 A/g. The experimental results also provide a new idea for the use of LDHs with a hollow polyhedral structure as an anode material[82].

Since 2011, the emergence of the MXene family headed by Ti_3C_2 has promoted the selection of electrode materials for alkali metal ion batteries. MXene has many advantages such as a large specific surface area, short ion diffusion path, and extremely small volume change during charging and discharging; however, its use as an electrode material is limited by its low theoretical capacity[83]. Zhao *et al.* combined a ZIF-67-polyhedron-derived negatively charged MXene framework with Co–Mo LDHs via a simple electrostatic self-assembly method (Fig. 10(a)). After thermal annealing, transition metal oxides (TMOs)@MXene (CoO/$Co_2Mo_3O_8$@MXene) composites were obtained (Fig. 10(b)), which were used as anodes of Li-ion batteries. The test results show that TMOs@MXene had a reversible capacity of 947.4 mA·h/g at a current density of 0.1 A/g, and it maintained a surprising specific capacity of 435.8 mA·h/g under 5 A/g (Fig. 10(c)). Even after 1200 cycles at 2 A/g, the capacity remained stable at 545 mA·h/g (Figs. 10(d) and 10(e)). This happens because the Co–Mo LDH derivatives compensate for the low theoretical capacity of MXene, and the CoO/$Co_2Mo_3O_8$ nanosheets greatly alleviate the agglomeration phenomenon of MXene. Moreover, the three-dimensional lamellar structure of MXene provides mechanical stability to the entire electrode system, overcoming the short cycle life problem caused by the volume expansion of internal TMOs@MXene. The advantages of both MXene and Co-Mo LDHs have been fully explored, showing another successful combination of LDHs and MXene[76].

3.2. Sodium-ion batteries

Compared with LIBs, sodium-ion batteries (SIBs) have more abundant reserves and uniform distribution; however, both batteries exhibit similar electrochemical behaviors. SIBs have gradually become more effective alternatives to LIBs[84]. However, the diameter of Na^+ is larger than that of Li^+, which makes it difficult to find suitable anode materials for Na^+ to shuttle freely[85, 86]. Zhao *et al.* used this property to synthesize SIB anode materials for the first time by intercalating Co-Fe LDH layers with two-dimensional nitrate columns. The CoFe-NO_3^- LDH half-cell exhibited an initial discharge capacity of 498 mA·h/g at a 1 A/g current density after testing (Fig. 11(a)). A high reversible capacity of 209 mA·h/g was still maintained after 200 charging–discharging cycles (Fig. 11(b)). Unlike the conversion reaction of LIB metal oxides, the excellent sodium-ion storage of the CoFe-NO_3^- LDH is attributed to the support of nitrate pillars within the Co-Fe LDH layer, which results in a large interlayer spacing. It exhibits a weaker Coulomb force than that of the LDH, which is favorable for the intercalation/deintercalation reaction of sodium ions. In addition, the low Na^+ diffusion barrier of 0.147 eV among the layers of the CoFe-NO_3^- LDH in the DFT calculation results indicates the applicability of LDHs as a superior and promising Na-ion conductor (Figs. 11(c)–11(e))[87].

The strong effect of microstructure stability on the performance of anode materials is obvious. Park *et al.* used ZIF-

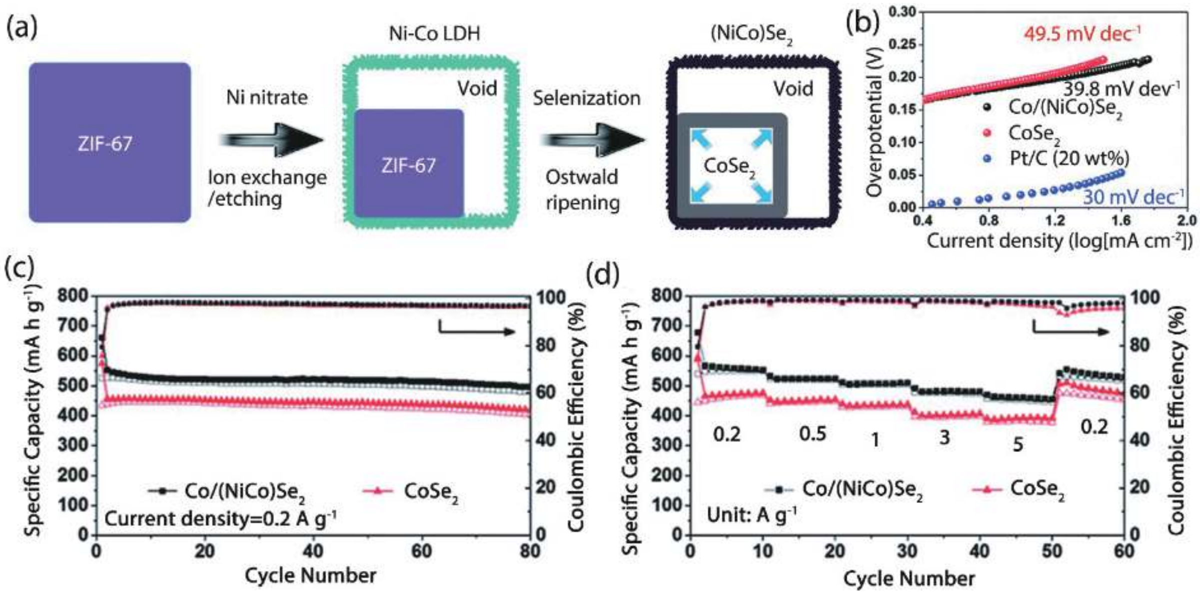

Fig. 12. (Color online) (a) The schematic illustration of box-in-box structure of Co/(NiCo)Se_2. (b) Tafel plots, (c) cycle stability and (d) rate performance of the Co/(NiCo)Se_2 nanocubes[77]. Copyright 2017, The Royal Society of Chemistry.

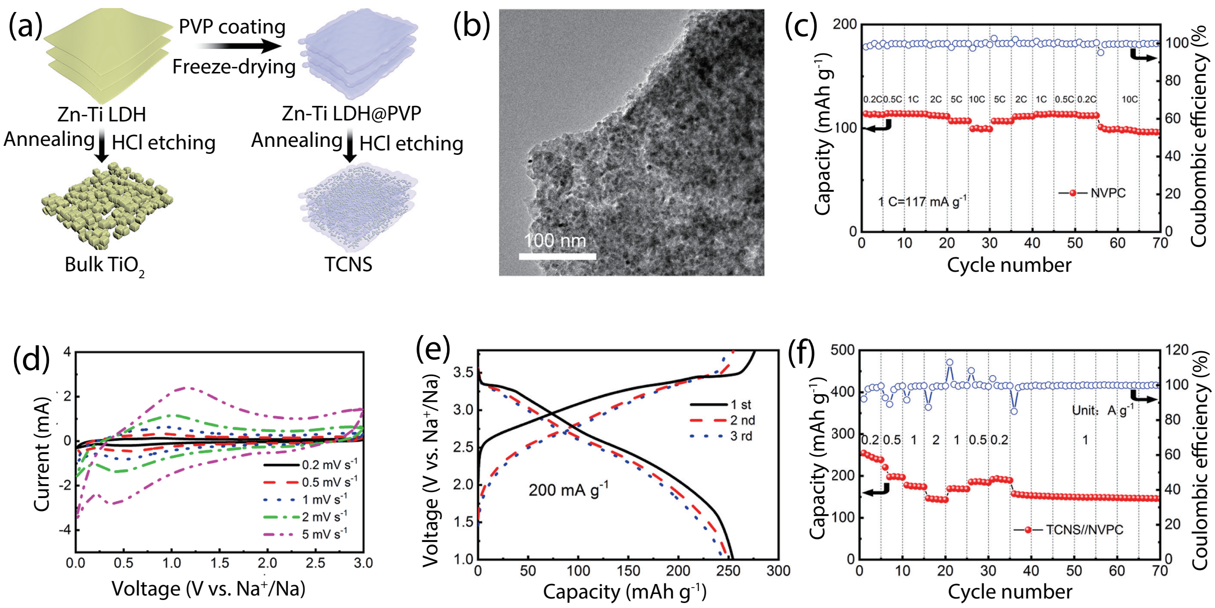

Fig. 13. (Color online) (a) Fabrication illustration of bulk TiO_2 and TCNS. (b) TEM images of Zn–Ti LDH, (c–f) ultrahigh stability and a specific capacity of Zn–Ti LDH@PV[88]. Copyright 2021, Elsevier Ltd.

67 nanocubes as precursors and etched them with nickel nitrate in ethanol to generate cubic ZIF-67/Ni-Co LDHs with a shell–core structure. Subsequently, under Ar/H_2 conditions, a box-in-box structure product, Co/(NiCo)Se_2, was obtained by the selenization of $CoSe_2$ in the core and (NiCo)Se_2 in the outer shell (Fig. 12(a)). Because of the unique configuration and the synergistic effect of multicomponent selenides, Co/(NiCo)Se_2 can serve as a good electrocatalyst for the hydrogen evolution reaction (HER), while acting as the anode for SIBs. The electrochemical test results show that the capacity remained at 497 mA·h/g after 80 cycles at a current density of 0.2 A/g, and the slope of its Tafel curve was only 39.8 mV/dec (Figs. 12(b) and 12(c)). Moreover, the rate performance was stable at a current density of 0.2–5 A/g (Fig. 12(d)). This work exploits the high capacity and excellent electrocatalytic properties of LDH derivatives[77].

In addition to the construction of a stable architecture, the combination of LDHs with carbon materials is a crucial approach for overcoming the significant capacity loss of batteries during cycling. In Chen's work, multiphase Mn-doped Ni sulfide (NMS) nanoparticles were prepared by the sulfidation method using the Ni–Mn LDH as the precursor and immobilized on the rGO surface as the final product of heterodoping. When used as an SIB anode in an ether-based electrolyte, it exhibits excellent rate capability (229.2 mA·h/g at 5.0 A/g) and cycling stability (206 mA·h/g after 2000 cycles at 0.5 A/g). The high-capacity properties of LDH nanomaterials further demonstrate the potential of metal sulfides as SIB anodes after being compounded with carbon materials[75].

Similarly, using the carbon composite method, Diao *et al.* used polyvinylpyrrolidone to carbon-coat a Zn–Ti LDH through annealing. Next, the zinc element in Zn–Ti LDH@PVP

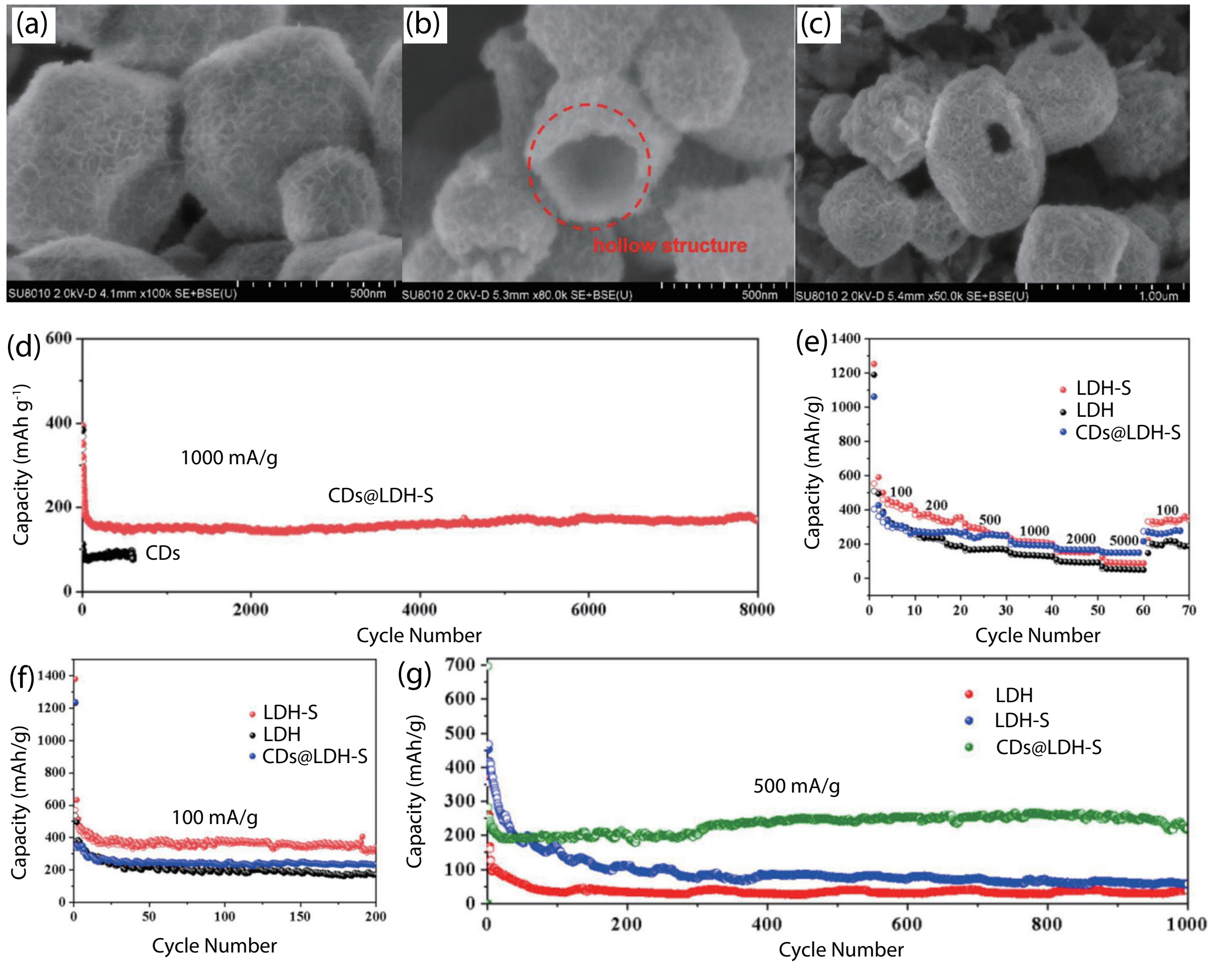

Fig. 14. (Color online) SEM images of (a) LDH, (b) LDH-S and (c) CDs@LDH-S. (d) Cycling performances of CDs and CDs@LDH-S at 1 A/g. (e) Rate performance at different current density of LDH, LDH-S and CDs@LDH-S. Cycling performance at (f) 0.1 A/g and (g) 0.5 A/g of LDH, LDH-S and CDs@LDH-S[94]. Copyright 2021, Elsevier Ltd.

was etched with hydrochloric acid to obtain ultrasmall TiO_2-nanoparticle-embedded carbon nanosheets (TCNS). The comparative experiments in the flow chart and SEM image demonstrate that the addition of PVP improves the preservation of the lamellar structure of the Zn–Ti LDH and prevents agglomeration (Fig. 13). Therefore, the composite exhibits great advantages for sodium storage, with ultrahigh stability and a specific capacity of 196.7 mA·h/g after 2000 cycles at 2 A/g. The research results show that the two-dimensional lamellar structure of LDHs is fragile, easy to agglomerate, and unstable in the absence of special protection. Upon overcoming these shortcomings, the application scope of such composites can be expanded[88].

3.3. Potassium-ion batteries

In the future, the depleting lithium resource deposits in the Earth's crust and the geopolitical concentrations of lithium may impede the expansion of lithium mining. However, the crustal contents of sodium and potassium are much higher than those of lithium, which suggests that rechargeable sodium and potassium batteries are attractive alternatives to LIBs[89, 90]. In the past decade, rechargeable potassium batteries (KIBs) have gained great attention. Compared with SIBs, KIBs have higher voltages (0.2–0.3 V) and a greater possibility of using graphite as an anode material[91–93]. However, the development of rechargeable KIBs is still in its infancy; there are only a few reports on the application of LDHs as electrode materials for KIBs. Here, we briefly summarize the applicability of LDHs in KIBs as represented by two recent research results.

In 2021, Yang *et al.* compared the performance of a Mg–Al LDH and Mg–Fe LDH as anodes for KIBs through comparative experiments. The test findings indicated that the specific capacity of the Mg–Al LDH without multivalent metal elements was only 195.2 mA·h/g at a current density of 0.1 A/g, but the initial coulombic efficiency was as high as 99.4%. In contrast, the Mg–Fe LDH with variable valence iron ions exhibited a potassium storage capacity of 371.6 mA·h/g at the same current density and cycle number, which is almost twice that of the Mg–Al LDH; the initial coulombic efficiency was 88.4%. This discrepancy is attributed to the difference in the potassium storage mechanism: The Mg–Al LDH/K battery utilizes the electric double-layer effect, while the Mg–Fe LDH/K battery mainly accomplishes potassium storage through the Faradaic reaction of conversion between Fe^{3+} and Fe^{2+}. The battery capacity retention rates of Mg–Fe LDH/K at current densities of 1, 2, 5, and 10 A/g were 60.9%, 51.3%, 42.9%, and 39.5%, respectively, in the rate performance test. These unsatisfactory results are attributed to the intrinsically low electrical conductivity of LDHs and the high surface activation energy of up to 79.5 kJ/mol, making it difficult for potassium ions to diffuse within the anode. This comparative experiment confirmed the feasibility of LDHs containing variable valence metal elements as an anode for KIBs. However, their low rate performance must be overcome for the application of LDHs as electrode materials for KIBs[94].

To alleviate this difficulty and to expand the application scope of LDHs, Jiang *et al.* developed Ni–Co LDH hollow nanocages utilizing ZIF-67 as a precursor in the same year. Subsequently, using an in situ sulfidation process, ultrafine metal sulfide nanoparticles were inserted into LDH nanocages to generate LDH-S (Figs. 14(a) and 14(b)). Consequently, the surface of LDH-S was modified with carbon dots (CDs), originating the final composite product CDs@LDH-S; its specific capacity was 188 mA·h/g after 8000 cycles at 1.0 A/g (Figs. 14(c) and 14(d)). Compared with the capacity retention of 70% for pure Ni–Co LDH and 88% for LDH-S, the capacity retention of CDs@LDH-S was as high as 96% at a current density of 0.1–5 A/g (Fig. 14(e)). The excellent performance can be attributed to the enhanced electrical conductivity owing to the interlayer confinement formed by ultrafine metal sulfides. The establishment of the three-dimensional cage-like structure alleviates the agglomeration phenomenon of the material during long-term cycling and compensates for the shortcomings of the traditional two-dimensional sheet structure of LDHs, which are fragile and easy to agglomerate. In addition, the performance comparison of LDH-S and CDs@LDH-S indicates that the addition of CDs can further improve the conductivity of the anode material, resulting in higher cycling stability at high current (Figs. 14(f) and 14(g)). This work has confirmed the applicability of LDHs as KIB electrodes toward energy storage, similar to those the LIBs and SIBs; the combination of carbon materials and LDHs can be utilized to create exceptional high-efficiency electrode materials, compensate for the low conductivity of LDHs, and provide a solution to overcome the significant performance degradation when LDHs with variable valence metal elements are used as anode materials[95].

4. Conclusion

This review of the research on LDHs toward the development of (flexible) supercapacitors and AIBs has placed emphasis is on how their bi-component or even multicomponent composition might further increase the cycle capacity and life of electrode materials, which promotes their application in flexible wearable electronic devices. This review also expounded the common synthesis strategies of LDHs, including the utilization of the core–shell structure, layered structure, hollow polyhedron, and carbon composites, as well as analyzed the various performance indicators of as-prepared electrochemical energy storage devices. The exciting results obtained thus far will guide follow-up research and development of LDHs.

Although the research on LDHs has been extensively conducted, there are still some shortcomings that need to be addressed. It is difficult to maintain a flexible electrode structure when LDHs are used as the electrode material in flexible supercapacitors owing to frequent and long-term bending deformation. Moreover, the energy density of LDH-based supercapacitors needs to be further improved. While LDHs in AIBs have a high theoretical capacity, some instability phenomena occur during charging and discharging, such as development of a fragile structure and agglomeration, which leads to low cycling stability and impede the guarantee of reversible capacity. Adjusting the metal type and interlayer spacing in the LDH host layer is often necessary to overcome these challenges. Optimization is achieved by combining LDH bases with conductive support materials and improving the surface morphology and internal structure of the LDHs.

In summary, it is still difficult to precisely regulate the structure of LDH-based materials and identify their active sites throughout the synthesis process. Under such circumstances, it is very important to develop cutting-edge characterization techniques to obtain a deep understanding of the microscale active-site characteristics of LDH materials and the synergistic effects between various constituents. Moreover, from the standpoint of environmental resources, attempts to design low-cost, high-quality, and environment-friendly LDH-based materials are critical for sustainable development[96, 97].

Acknowledgements

The authors sincerely acknowledge financial support from the National Natural Science Foundation of China (NSFC Grant No. 62174152).

References

[1] Tang Y, Li X, Lv H, et al. Integration designs toward new-generation wearable energy supply-sensor systems for real-time health monitoring: A minireview. InfoMat, 2020, 2, 1109
[2] Liu L, Zhao H, Lei Y. Advances on three-dimensional electrodes for micro-supercapacitors: A mini-review. InfoMat, 2019, 1, 71
[3] Zhang Y, Cao J, Yuan Z, et al. TiVCTx MXene/chalcogenide heterostructure-based high-performance magnesium-ion battery as flexible integrated units. Small, 2022, 2202313
[4] Wang H, Zhang N, Li S M, et al. Metal-organic framework composites for energy conversion and storage. J Semicond, 2020, 41, 091707
[5] Baig N, Sajid M. Applications of layered double hydroxides based electrochemical sensors for determination of environmental pollutants: A review. Trends Environ Anal Chem, 2017, 16, 1
[6] Dong K, Wang Z L. Self-charging power textiles integrating energy harvesting triboelectric nanogenerators with energy storage batteries/supercapacitors. J Semicond, 2021, 42, 101601
[7] Dong K, Hu Y, Yang J, et al. Smart textile triboelectric nanogenerators: Current status and perspectives. MRS Bulletin, 2021, 46, 512
[8] Li M, Lu J, Chen Z, et al. 30 years of lithium-ion batteries. Adv Mater, 2018, 30, 1800561
[9] Li X, Du D, Zhang Y, et al. Layered double hydroxides toward high-performance supercapacitors. J Mater Chem A, 2017, 5, 15460
[10] Zhang Y, Cao J, Li J, et al. Self-assembled Cobalt-doped NiMn-layered double hydroxide (LDH)/V_2CTx MXene hybrids for advanced aqueous electrochemical energy storage properties. Chem Eng J, 2022, 430, 132992
[11] Yan A L, Wang X C, Cheng J P. Research progress of NiMn layered double hydroxides for supercapacitors: A review. Nanomaterials, 2018, 8, 747
[12] Shou Q, Cheng J, Zhang L, et al. Synthesis and characterization of a nanocomposite of goethite nanorods and reduced graphene oxide for electrochemical capacitors. J Solid State Chem, 2012, 185, 191
[13] Meng H, Xi W, Ren Z, et al. Solar-boosted electrocatalytic oxygen evolution via catalytic site remodelling of CoCr layered double hydroxide. Appl Catal B, 2021, 284, 119707
[14] Fan G, Li F, Evans D G, et al. Catalytic applications of layered double hydroxides: recent advances and perspectives. Chem Soc Rev, 2014, 43, 7040
[15] Ma J, Chen Y, He G, et al. A robust H-transfer redox mechanism de-

termines the high-efficiency catalytic performance of layered double hydroxides. Appl Catal B, 2021, 285, 119806
[16] Zhao S, Ran W, Lou Z, et al. Neuromorphic-computing-based adaptive learning using ion dynamics in flexible energy storage devices. Natl Sci Rev, 2022, 9, nwac158
[17] Li L, Zhao S, Ran W, et al. Dual sensing signal decoupling based on tellurium anisotropy for VR Interaction and neuro-reflex system application. Nat Commun, 2022, 13, 5975
[18] Jiang S D, Bai Z M, Tang G, et al. Synthesis of mesoporous silica@Co-Al layered double hydroxide spheres: layer-by-layer method and their effects on the flame retardancy of epoxy resins. ACS Appl Mater Interfaces, 2014, 6, 14076
[19] Xu S, Li S Y, Zhang M, et al. Fabrication of green alginate-based and layered double hydroxides flame retardant for enhancing the fire retardancy properties of polypropylene. Carbohydr Polym, 2020, 234, 115891
[20] Ameena Shirin V K, Sankar R, Johnson A P, et al. Advanced drug delivery applications of layered double hydroxide. J Control Release, 2021, 330, 398
[21] Xu T, Zhang J, Chi H, et al. Multifunctional properties of organic-inorganic hybrid nanocomposites based on chitosan derivatives and layered double hydroxides for ocular drug delivery. Acta Biomater, 2016, 36, 152
[22] Cao J, Wang L, Li D, et al. $Ti_3C_2T_x$ MXene conductive layer supported bio-derived $Fe_{x-1}Se_x$/MXene/carbonaceous nanoribbons for high-performance half/full sodium-ion and potassium-ion batteries. Adv Mater, 2021, 33, 2101535
[23] Zhang Y, Wang L, Zhao L, et al. Flexible self-powered intergrated sensing system with 3D periodic ordered black phosphorus @MXene thin-film. Adv Mater, 2021, 33, 2007890
[24] Laipan M, Yu J, Zhu R, et al. Functionalized layered double hydroxides for innovative applications. Mater Horiz, 2020, 7, 715
[25] Mittal J. Recent progress in the synthesis of layered double hydroxides and their application for the adsorptive removal of dyes: A review. J Environ Manage, 2021, 295, 113017
[26] Sarfraz M, Shakir I. Recent advances in layered double hydroxides as electrode materials for high-performance electrochemical energy storage devices. J Energy Storage, 2017, 13, 103
[27] Yu J, Wang Q, O'Hare D, et al. Preparation of two dimensional layered double hydroxide nanosheets and their applications. Chem Soc Rev, 2017, 46, 5950
[28] Tao H, Fan Q, Ma T, et al. Two-dimensional materials for energy conversion and storage. Prog Mater Sci, 2020, 111, 100637
[29] Baker C O, Huang X, Nelson W, et al. Polyaniline nanofibers: broadening applications for conducting polymers. Chem Soc Rev, 2017, 46, 1510
[30] Liu L, Niu Z, Chen J. Unconventional supercapacitors from nanocarbon-based electrode materials to device configurations. Chem Soc Rev, 2016, 45, 4340
[31] Chen C, Zhang Y, Li Y, et al. Wood low tortuosity, aqueous, biodegradable supercapacitors with ultra-high capacitance. Energy Environl Sci, 2017, 10, 538
[32] Gao X, Wang P, Pan Z, et al. Recent progress in two-dimensional layered double hydroxides and their derivatives for supercapacitors. ChemSusChem, 2020, 13, 1226
[33] Ma L, Liu R, Niu H, et al. Flexible and freestanding supercapacitor electrodes based on nitrogen-doped carbon networks/graphene/bacterial cellulose with ultrahigh areal capacitance. ACS Appl Mater Interfaces, 2016, 8, 33608
[34] Liang J, Feng Y, Liu L, et al. All-printed solid-state supercapacitors with versatile shapes and superior flexibility for wearable energy storage. J Mater Chem A, 2019, 7, 15960
[35] Dong K, Peng X, Cheng R, et al. Advances in high-performance autonomous energy and self-powered sensing textiles with novel 3D fabric structures. Adv Mater, 2022, 34, 2109355
[36] Dong K, Peng X, Cheng R, et al. Smart textile triboelectric nanogenerators: Prospective strategies for improving electricity output performance. Nanoenergy Adv, 2022, 2, 133
[37] Jin S, Allam O, Jang S, et al. Covalent organic frameworks: Design and applications in electrochemical energy storage devices. InfoMat, 2022, 4, e12277
[38] Zhao M, Zhao Q, Li B, et al. Recent progress in layered double hydroxide based materials for electrochemical capacitors: design, synthesis and performance. Nanoscale, 2017, 9, 15206
[39] Lu Z, Qian L, Tian Y, et al. Ternary NiFeMn layered double hydroxides as highly-efficient oxygen evolution catalysts. Chem Commun, 2016, 52, 908
[40] Wang R, Yao M, Niu Z. Smart supercapacitors from materials to devices. InfoMat, 2020, 2, 2148
[41] Lan Y, Zhao H, Zong Y, et al. Phosphorization boosts the capacitance of mixed metal nanosheet arrays for high performance supercapacitor electrodes. Nanoscale, 2018, 10, 11775
[42] Yuan Z, Cao J, Valerii S, et al. MXene-bonded hollow MoS_2/carbon sphere strategy for high-performance flexible sodium ion storage. Chem Eng J, 2022, 430, 132755
[43] Li X, Shen J, Sun W, et al. A super-high energy density asymmetric supercapacitor based on 3D core –shell structured NiCo-layered double hydroxide@carbon nanotube and activated polyaniline-derived carbon electrodes with commercial level mass loading. J Mater Chem A, 2015, 3, 13244
[44] Xuan X, Qian M, Han L, et al. In-situ growth of hollow NiCo layered double hydroxide on carbon substrate for flexible supercapacitor. Electrochimica Acta, 2019, 321, 134710
[45] Lau C N, Bao W, Velasco J. Properties of suspended graphene membranes. Mater Today, 2012, 15, 238
[46] Castro Neto A H, Guinea F, Peres N M R, et al. The electronic properties of graphene. Rev Mod Phys, 2009, 81, 109
[47] Kiran S K, Shukla S, Struck A, et al. Surface enhanced 3D rGO hybrids and porous rGO nano-networks as high performance supercapacitor electrodes for integrated energy storage devices. Carbon, 2020, 158, 527
[48] Chen T, Dai L. Flexible supercapacitors based on carbon nanomaterials. J Mater Chem A, 2014, 2, 10756
[49] Senthilkumar S T, Wang Y, Huang H. Advances and prospects of fiber supercapacitors. J Mater Chem A, 2015, 3, 20863
[50] Xu P, Gu T, Cao Z, et al. Carbon nanotube fiber based stretchable wire-shaped supercapacitors. Adv Energy Mater, 2014, 4, 1300759
[51] Le T S, Truong T K, Huynh V N, et al. Synergetic design of enlarged surface area and pseudo-capacitance for fiber-shaped supercapacitor yarn. Nano Energy, 2020, 67, 104198
[52] Li L, Zhou Y, Zhou H, et al. N/P codoped porous carbon/one-dimensional hollow tubular carbon heterojunction from biomass inherent structure for supercapacitors. ACS Sustain Chem Eng, 2018, 7, 1337
[53] Qin F, Tian X, Guo Z, et al. Asphaltene-based porous carbon nanosheet as electrode for supercapacitor. ACS Sustain Chem Eng, 2018, 6, 15708
[54] Tabassum H, Zou R, Mahmood A, et al. A universal strategy for hollow metal oxide nanoparticles encapsulated into B/N Co-doped graphitic nanotubes as high-performance lithium-ion battery anodes. Adv Mater, 2018, 30, 1705441
[55] Lee J, Kitchaev D A, Kwon D H, et al. Reversible $Mn^{(2+)}$/$Mn^{(4+)}$ double redox in lithium-excess cathode materials. Nature, 2018, 556, 185
[56] Chen H C, Qin Y, Cao H, et al. Synthesis of amorphous nickel–cobalt–manganese hydroxides for supercapacitor-battery hybrid energy storage system. Energy Storage Mater, 2019, 17, 194
[57] Chen J, Wang X, Wang J, et al. Sulfidation of NiMn-layered double hydroxides/graphene oxide composites toward supercapacitor electrodes with enhanced performance. Adv Energy Mater, 2016, 6, 1501745
[58] Cao J, Li J, Li L, et al. Mn-doped Ni/Co LDH nanosheets grown on the natural N-dispersed PANI-derived porous carbon template for a flexible asymmetric supercapacitor. ACS Sustain Chem Eng,

2019, 7, 10699
[59] Li M, Jijie R, Barras A, et al. NiFe layered double hydroxide electrodeposited on Ni foam coated with reduced graphene oxide for high-performance supercapacitors. Electrochimica Acta, 2001, 302, 1
[60] Yang S, Liu Y, Hao Y, et al. Oxygen-vacancy abundant ultrafine Co_3O_4/graphene composites for high-rate supercapacitor electrodes. Adv Sci, 2018, 5, 1700659
[61] Yin B, Zhang S, Jiao Y, et al. Facile synthesis of ultralong MnO_2 nanowires as high performance supercapacitor electrodes and photocatalysts with enhanced photocatalytic activities. CrystEngComm, 2014, 16, 9999
[62] Yin B, Zhang S, Jiang H, et al. Phase-controlled synthesis of polymorphic MnO_2 structures for electrochemical energy storage. J Mater Chem A, 2015, 3, 5722
[63] Zhao Y, He J, Dai M, et al. Emerging CoMn-LDH@MnO_2 electrode materials assembled using nanosheets for flexible and foldable energy storage devices. J Energy Chem, 2020, 45, 67
[64] Wang Y, Yang H, Lv H, et al. High performance flexible asymmetric supercapacitor constructed by cobalt aluminum layered double hydroxide@nickel cobalt layered double hydroxide heterostructure grown in-situ on carbon cloth. J Colloid Interface Sci, 2022, 610, 35
[65] Li Y, Yan X, Zhang W, et al. Hierarchical micro-nano structure based NiCoAl-LDH nanosheets reinforced by $NiCo_2S_4$ on carbon cloth for asymmetric supercapacitor. J Electroanal Chem, 2022, 905, 115982
[66] Ni C S, Liu S F, Lee J F, et al. Binder-free NiCoFe layered double hydroxide nanosheets for flexible energy storage devices with high-rate-retention characteristics. Electrochimica Acta, 2021, 384, 138415
[67] He F, Hu Z, Liu K, et al. Facile fabrication of GNS/NiCoAl-LDH composite as an advanced electrode material for high-performance supercapacitors. J Solid State Electr, 2014, 19, 607
[68] Bai X, Liu Q, Liu J, et al. All-solid state asymmetric supercapacitor based on NiCoAl layered double hydroxide nanopetals on robust 3D graphene and modified mesoporous carbon. Chem Eng J, 2017, 328, 873
[69] Xu J, Gai S, He F, et al. Reduced graphene oxide/$Ni_{1-x}Co_x$Al-layered double hydroxide composites: preparation and high supercapacitor performance. Dalton Trans, 2014, 43, 11667
[70] He X, Liu Q, Liu J, et al. Hierarchical $NiCo_2O_4$@NiCoAl-layered double hydroxide core/shell nanoforest arrays as advanced electrodes for high-performance asymmetric supercapacitors. J Alloys Compd, 2017, 724, 130
[71] Wang X, Li H, Li H, et al. Heterostructures of Ni–Co–Al layered double hydroxide assembled on V4C3MXene for high-energy hybrid supercapacitors. J Mater Chem A, 2019, 7, 2291
[72] Gao X, Liu X, Wu D, et al. Significant role of Al in ternary layered double hydroxides for enhancing electrochemical performance of flexible asymmetric supercapacitor. Adv Funct Mater, 2019, 29, 1903879
[73] Poudel M B, Kim H J. Confinement of Zn-Mg-Al-layered double hydroxide and α-Fe_2O_3 nanorods on hollow porous carbon nanofibers: A free-standing electrode for solid-state symmetric supercapacitors. Chem Eng J, 2022, 429, 132345
[74] Xu S F, Sun M X, Wang Q, et al. Recent progress in organic electrodes for zinc-ion batteries. J Semicond, 2020, 41, 091704
[75] Chen J, Li S, Qian K, et al. NiMn layered double hydroxides derived multiphase Mn-doped Ni sulfides with reduced graphene oxide composites as anode materials with superior cycling stability for sodium ion batteries. Mater Today Energy, 2018, 9, 74
[76] Zhao X, Xu H, Hui Z. Electrostatically assembling 2D nanosheets of MXene and MOF-derivatives into 3D hollow frameworks for enhanced lithium storage. Small, 2019, 15, e1904255
[77] Park S K, Kim J K, Kang Y. Metal–organic framework-derived $CoSe_2$/(NiCo)Se_2 box-in-box hollow nanocubes with enhanced electrochemical properties for sodium-ion storage and hydrogen evolution. J Mater Chem A, 2017, 5, 18823
[78] Zhu H, Sha M, Zhao H, et al. Highly-rough surface carbon nanofibers film as an effective interlayer for lithium–sulfur batteries. J Semicond, 2020, 41, 092701
[79] Wang J, Wang L, Chen X, et al. Chemical power source based on layered double hydroxides. J Solid State Electr, 2015, 19, 1933
[80] Liu J, Li Y, Huang X, et al. Layered double hydroxide nano- and microstructures grown directly on metal substrates and their calcined products for application as Li-ion battery electrodes. Adv Funct Mater, 2008, 18, 1448
[81] Zhang J, Yang Z, Qiu J, et al. Design and synthesis of nitrogen and sulfur co-doped porous carbon via two-dimensional interlayer confinement for a high-performance anode material for lithium-ion batteries. J Mater Chem A, 2016, 4, 5802
[82] Lu Y, Du Y, Li H. Template-sacrificing synthesis of Ni-Co layered double hydroxides polyhedron as advanced anode for lithium ions battery. Front Chem, 2020, 8, 581653
[83] Hantanasirisakul K, Gogotsi Y. Electronic and optical properties of 2D transition metal carbides and nitrides (MXenes). Adv Mater, 2018, 30, e1804779
[84] Delmas C. Sodium and sodium-ion batteries: 50 years of research. Adv Energy Mater, 2018, 8, 1703137
[85] Okamoto K, Iyi N, Sasaki T. Factors affecting the crystal size of the MgAl-LDH (layered double hydroxide) prepared by using ammonia-releasing reagents. Appl Clay Sci, 2007, 37, 23
[86] Inayat A, Klumpp M, Schwieger W, et al. The urea method for the direct synthesis of ZnAl layered double hydroxides with nitrate as the interlayer anion. Appl Clay Sci, 2011, 51, 452
[87] Zhao Y, Sun T, Yin Q, et al. Discovery of a new intercalation-type anode for high-performance sodium ion batteries. J Mater Chem A, 2019, 7, 15371
[88] Diao Z, Wang Y, Zhao D, et al. Ultra-small TiO_2 nanoparticles embedded in carbon nanosheets for high-performance sodium storage. Chem Eng J, 2021, 417, 127928
[89] Zhang W, Yin J, Wang W, et al. Status of rechargeable potassium batteries. Nano Energy, 2021, 83, 105792
[90] Eftekhari A, Jian Z, Ji X. Potassium secondary batteries. ACS Appl Mater Interfaces, 2017, 9, 4404
[91] Zhou J, Liu Y, Zhang S, et al. Metal chalcogenides for potassium storage. InfoMat, 2020, 2, 437
[92] Li C, Li P, Yang S, Zhi C Y. Recently advances in flexible zinc ion batteries. J Semicond, 2021, 42, 101603
[93] Deng S, Cheng S, Liu M, et al. Modulating magnetic properties by tailoring in-plane domain structures in hexagonal $YMnO_3$ films. ACS Appl Mater Interfaces, 2016, 8, 25379
[94] Yang Q, Lv K, Liang L, et al. Layered double hydroxides as high-performance anode material for potassium ion battery. J Alloys Compd, 2021, 882, 160711
[95] Jiang Q, Wang L, Zhao W, et al. Carbon dots decorated on the ultrafine metal sulfide nanoparticles implanted hollow layered double hydroxides nanocages as new-type anodes for potassium-ion batteries. Chem Eng J, 2022, 433, 133539
[96] Ma X H, Jiang Z F, Lin Y J. Flexible energy storage devices for wearable bioelectronics. J Semicond, 2021, 42, 101602
[97] Zhao C, Wang Z J, Shu D J, et al. Preface to the special issue on challenges and possibilities of energy storage. J Semicond, 2020, 41, 090101

Qifeng Lin is currently a B.S. candidate at College of Electronic Science and Engineering of Jilin University, Changchun, China. His research interests mainly focus on layered double hydroxides materials-based flexible energy storage devices.

Lili Wang is a professor in the Institute of Semiconductors, Chinese Academy of Sciences, China. She earned her B.S. degree in Chemistry and Ph.D degree in Microelectronics and Solid State Electronics from Jilin University in 2014. Her current research interests focus on the semiconductor multimode intelligent sensing integrated system.